

# Development of a Bright Polychromator for Thomson Scattering Measurements

Akira EJIRI, Takashi YAMAGUCHI, Junichi HIRATSUKA, Yuichi TAKASE, Makoto HASEGAWA<sup>1)</sup> and Kazumichi NARIHARA<sup>2)</sup>

*Graduate School of Frontier Sciences, The University of Tokyo, Kashiwa 277-8561, Japan*

<sup>1)</sup>*Research Institute for Applied Mechanics, Kyushu University, Kasuga 816-8580, Japan*

<sup>2)</sup>*National Institute for Fusion Science, 322-6 Oroshi-cho, Toki 509-5292, Japan*

(Received 7 December 2009 / Accepted 4 March 2010)

A bright polychromator for compact, efficient YAG Thomson scattering measurement was designed on the basis of ray-tracing calculations. The optical input of the polychromator is a 2-mm-diameter optical fiber with a numerical aperture of 0.37. High refractive index glass lenses with monolayer anti-reflection coatings were used to reduce aberration effects and achieve good efficiency. A fast, low-noise detection system consisting of an avalanche photodiode and operational amplifiers was designed and tested using YAG laser pulses; the measured full width at half maximum (FWHM) of the laser pulse was 10 ns. The measured noise was dominated by the thermal noise of the input resistance  $R$  ( $= 470 \Omega$ ) when the signal was low, and the shot noise became dominant when the number of detected photons was greater than about 500.

© 2010 The Japan Society of Plasma Science and Nuclear Fusion Research

**Keywords:** Thomson scattering, forward-backward scattering, polychromator, avalanche photodiode, spherical tokamak, non-inductive start-up, low density plasma

DOI: 10.1585/pfr.5.S2082

## 1. Introduction

Thomson scattering is a standard technique for electron temperature and density measurement. Since the scattering cross-section is very small, an efficient system is necessary to measure low density plasmas. Non-inductive start-up of a spherical tokamak (ST) is one such case, where the plasma is generated by RF waves, and the densities are as low as  $10^{17} \text{ m}^{-3}$  in recent experiments. Electron temperature and density measurements are critical for studying the equilibrium during ST formation phase [1] and the coupling of the RF waves and the plasma. In order to measure the temperature and density of such low density plasmas, a Thomson scattering system should be very efficient.

In the TST-2 ST device, a thick core (2 mm in diameter), large numerical aperture ( $NA = 0.37$ ) fiber, Newtonian collecting optics are used to form a compact, efficient system [2]. Ohmic discharge plasmas with electron densities  $\sim 1 \times 10^{19} \text{ m}^{-3}$  are measured with a good S/N ratio ( $\sim 10$ ). However, the polychromator, on loan from the National Institute for Fusion Science, was designed for an optical fiber with  $NA = 0.22$  [3], and it is not optimized for a fiber with  $NA = 0.37$ . To measure the low density non-inductive plasmas, we are developing a new polychromator optimized for a large- $NA$  optical fiber. The first part of the paper describes the optics design determined by ray-tracing calculations. We found that spherical lenses made of high refractive index glass are useful for achieving high

efficiency.

In addition to optimizing the polychromator, we are planning to use a multiple-path scattering scheme (based on a confocal spherical mirror cavity), from which a train of scattering pulses is expected. By resolving each pulse or accumulating all the pulses, we can improve the S/N ratio. When we apply this scenario to a forward-backward scattering configuration, these two types of scattering occur alternatively. In this case, we must resolve each pulse, because those two different configurations have different scattering vectors. Moreover, we can take advantage of the differences to distinguish between parallel and perpendicular temperatures. In collisionless ST plasmas, we can expect a large anisotropy in the pressure, due to the large mirror effect. Therefore, the multiple-path scheme with a forward-backward scattering configuration which we are planning to install on the TST-2 and the QUEST ST devices [4], is very useful. The cavity length (i.e., the distance between the laser injection and exit ports) is about 6 m; thus, the time difference between each pair of pulses is about 20 ns. A very fast response is required for the detector and the preamplifier. We use an avalanche photodiode (APD) with a large sensitive diameter (3 mm) and small terminal capacitance ( $C = 8 \text{ pF}$ ) as the detector. A photomultiplier tube (PMT) is another candidate for the detector. It has a fast response, high gain, low normalized dark current. However, its quantum efficiency is very low for infrared light and is also low for wavelengths around the second-harmonic light of the YAG laser. As a result,

author's e-mail: ejiri@k.u-tokyo.ac.jp

PMTs are not useful as long as the number of incident photons is not too small (e.g., ~ 100). The last part of the paper describes the design and tests of a prototypical detection system.

## 2. Polychromator Optics Design

Recent development in fiber fabrication technology enables a large *NA* fiber. Fibers with *NA* as large as 0.37 are used in several polychromators [5–7]. Reference [5] compared several designs for a 3-mm-diameter fiber bundle with *NA* = 0.37, and showed that losses of several tens of percent can easily occur for a compact system. In general, designing a compact, bright optical system is not easy. The brightness is measured through etendue, which is the product of the sensitive area and the acceptable solid angle on the area. Since we are going to increase the *NA* of an optical fiber while keeping its diameter constant, the etendue of the polychromator should be increased. The easiest way to do this is to use much larger diameter optical elements, but it is impractical in our case. In addition, the following feature of the present polychromator design should be considered. The present polychromator adopts an asymmetric relay configuration, in which the odd and even channels are asymmetric (Fig. 1). In this configuration, the number of relay lenses is reduced, but vignetting is more likely. Therefore, numerical estimation of such loss is necessary for each design.

In order to increase the designed *NA* from 0.22 to 0.37, small F-number lenses should be used. However, standard small F-number lenses have large aberration. Aspheric lenses or high refractive index glass can be used to address this problem. After ray-tracing calculations, we selected the latter, choosing SF11 glass ( $n = 1.76$  @ 1000 nm), and a satisfactory design was found (Fig. 1). The polychromator has six detectors as the six wavelength channels. The efficiency, which is the ratio of rays starting from the fiber exit to those reaching a detector, is calculated for each channel. We took the minimum among the six channel efficiencies as the measure of the goodness of the design. In the calculation, we neglected surface reflections and assumed ideal performance for the interference filters. We also introduced artificial reduction of the diameters of the lenses and detectors (by about 10%) to preserve the margins for various practical errors.

Figure 2 shows contour maps of efficiency in the plane of the two focal lengths. Three maps are shown for three focal lengths of the relay lens. The encircled + symbol represents the determined design point, which is not the optimum in terms of efficiency. We selected slightly longer focal lengths for the collimator and the detector lenses to reduce the curvature radii of the lens surfaces. Due to the small F-number design, the curvature can be significant, even though we use high refractive index glass. The curvature induces off-normal incidence angles to the lens surfaces, degrading the performance of the anti-reflection

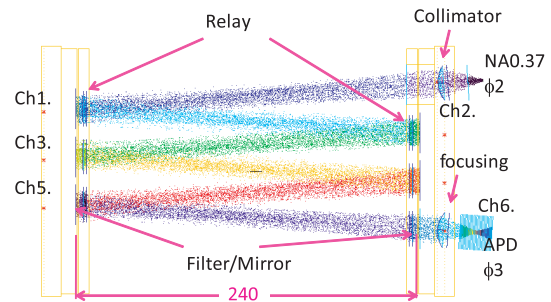


Fig. 1 Layout of the optics and rays in the polychromator.

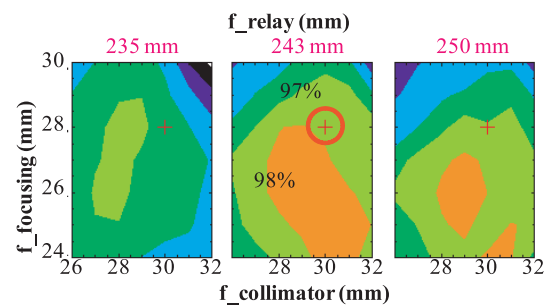


Fig. 2 Contour plots of the efficiency as a function of the two focal lengths. Three figures with different focal lengths of the relay lens are shown. Encircled + symbol represents the determined design point.

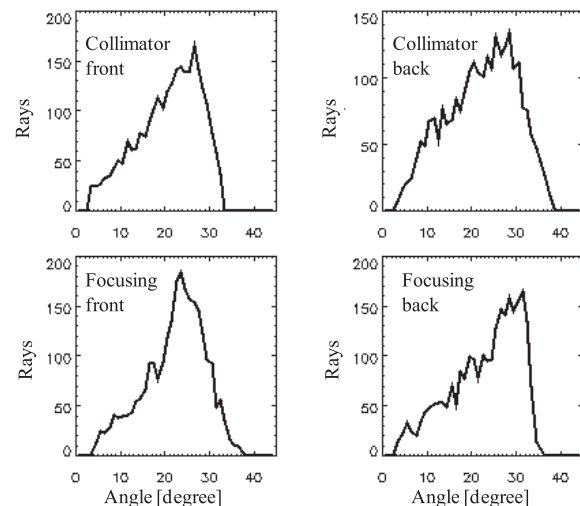


Fig. 3 Distribution of the incidence or exit angle of rays on the collimator and focusing lenses.

(AR) coating. Figure 3 shows the distribution of the air-side incidence or exit angles of rays. The distributions are well balanced between the four surfaces, and this balance also ensures less aberration.

Several concerns should be addressed when using high refractive index glass. One is the AR coating, and the other is chromatic aberration. Due to the high refractive index, the normal incidence reflectivity for bare SF11 is 8%,

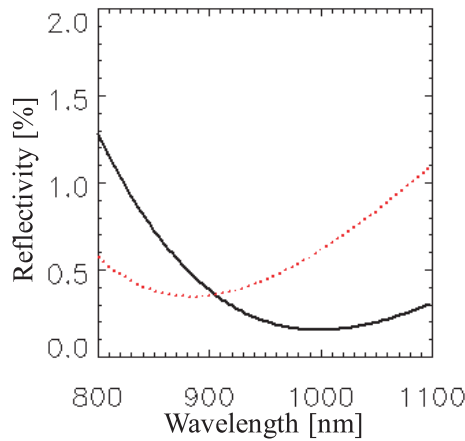


Fig. 4 Reflectivity of monolayer MgF<sub>2</sub> AR coating on SF11 for incidence angles of 0° (solid curve) and 40° (dashed curve) as a function of wavelength.

while that for BK7 is 4% at 1000 nm. However, a monolayer MgF<sub>2</sub> AR coating on SF11 yields a very small reflectivity of about 0.2%, because of the amplitude matching condition for the refractive indices. Figure 4 shows the reflectivity of the monolayer AR coating for incidence angles of 0 and 40°. Although a multilayer AR coating yields better performance, a monolayer AR coating is preferable for the broad angle distributions shown in Fig. 3. In addition, a weaker curvature of the lens surface is preferable, because it is difficult to control the AR coating's thickness on curved surfaces.

The chromatic aberration effect is not serious. The ray-tracing calculation indicates that the efficiency varies by ± 1% in the wavelength range 900-1050 nm. The degree of chromatic aberration is represented by the Abbe number in the visible range. SF11 is known to have a small Abbe number (i.e., significant chromatic aberration), but when we calculate a similar value in the infrared range, the value is very large, and the chromatic aberration is negligible as a result.

### 3. Design and Testing of a Detection System

In order to measure low density plasmas, a low-noise detection system should be developed. On the other hand, the multiple-path Thomson scattering scheme requires a very fast response. Thermal noise from the input resistance (i.e., current to voltage conversion resistance) and shot noise are the main noise sources. In general, high resistance is preferable to suppress the thermal noise, but it tends to result in a slow response. Therefore, we expected to have to balance noise suppression and fast response by optimizing the value of the resistance. However, we found that the thermal noise does not depend on the resistance, and we chose a very small resistance of 470 Ω.

We selected an APD (Hamamatsu Photonics, S8890-30) for the detector. This APD has a large sensitive di-

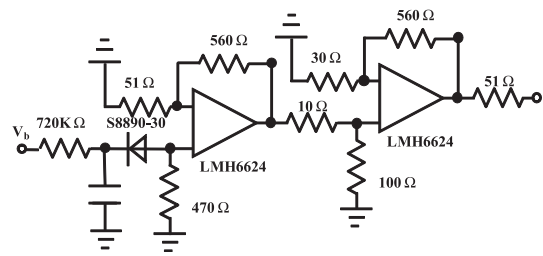


Fig. 5 Circuit diagram of the detector unit.

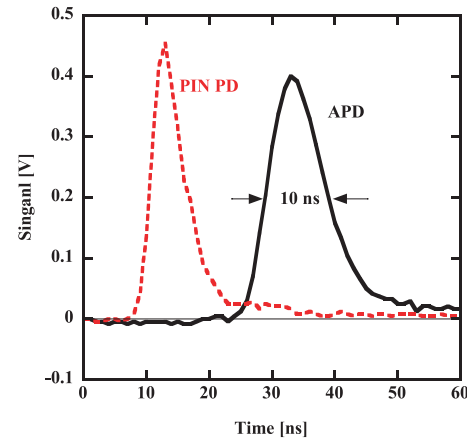


Fig. 6 Signal waveform of the prototypical APD detector system (solid curve) illuminated by a YAG laser pulse. Signal waveform of a PIN Si photodiode monitor (dashed curve) is also plotted.

ameter of 3 mm, and a small terminal capacitance of 8 pF. The former is necessary for a bright polychromator, and the latter is preferable for a fast response. Figure 5 shows a circuit diagram of the detector unit, including an APD and a two-stage noninverting amplifier composed of two low-noise operational amplifiers (National Semiconductor, LMH6624). We use the DC operational amplifiers (op-amps), because DC component is necessary to determine whether the signal is saturated. Using a low input resistance ( $R = 470 \Omega$ ), a fast response of the order of  $RC$  ( $= 4 \text{ ns}$ ) is expected.

The response of the detector unit was measured by detecting a YAG laser pulse. In Fig. 6, the waveform of the signal of a prototypical detector system is plotted. The FWHM of the pulse waveform is 10 ns, which is broader than a monitor PIN Si photodiode signal, but it is sufficiently short for the multiple-path scattering scheme. When the intensity is large the output signal may saturate. For this system, the signals start to saturate when the amplitude exceeds 2.5 V, which corresponds to the detected photon number of 40000.

Here, we estimate the theoretical noise of the detector system. As a measure of the noise, we calculate the relative error in the detected photon number  $\Delta N/N$ . In the estimation, we use nominal (i.e., typical) values for vari-

ous parameters of the APD and the op-amps. The thermal noise  $\Delta N_R$  is written as

$$\Delta N_R = \frac{\Delta i T_w}{eM} = \sqrt{\frac{4kT\Delta f}{R} \frac{T_w}{eM}} = \sqrt{\frac{2kTT_w}{R} \frac{1}{eM}}, \quad (1)$$

where  $\Delta i$  is the current noise,  $e$  is the electron charge,  $M$  ( $= 100$ ) is the avalanche gain of the APD,  $kT$  ( $= 300$  K) is the temperature, and  $\Delta f \equiv 1/2T_w$  and  $T_w$  ( $= 30$  ns) are the frequency bandwidth and the corresponding integration time, respectively. Shot noise arises from probabilistic detection, following a Poisson distribution. For APDs, an enhancement factor of  $\sqrt{M^x}$  (with  $x \sim 0.3$ ) should be used. The resultant shot noise  $\Delta N_S$  is written as

$$\Delta N_S = \sqrt{NM^x}. \quad (2)$$

The dark current  $i_D$  ( $\sim 15$  nA) is another noise source written as

$$\Delta N_D = \frac{T_w}{eM} \sqrt{2e i_D \Delta f M^x} = \sqrt{\frac{i_D T_w M^x}{eM^2}}. \quad (3)$$

For the circuit shown in Fig. 5, the thermal noise is  $\Delta N_R \sim 45$  photons, while the dark current noise is  $\Delta N_D \sim 1$  photon. Therefore, the dark current noise can be neglected.

In addition to the thermal noise, op-amps have input voltage noise  $e_n$  and input current noise  $i_n$ . The total amplifier noise is the sum of these components, written as

$$\Delta V = \sqrt{(e_n^2 + (i_n R)^2 + 4kTR)} \Delta f. \quad (4)$$

According to this equation, there is a resistance range in which the thermal noise dominates the other noises. The resistance range for the op-amp LMH6624 is from 33  $\Omega$  to 6 k $\Omega$ , and the present amplifier noise is dominated by the thermal noise from the resistance  $R = 470 \Omega$ . In other words, for a given input resistance, we should select an appropriate op-amp so that the circuit noise is dominated by thermal noise.

The shot noise obviously becomes dominant at a large number of detected photons  $N$ . Shot noise is often measured as a function of incident light intensity to obtain the absolute sensitivity of an optical detector [8, 9]. A similar measurement was performed and compared with the theoretical estimates in Eqs. (1) and (2). Figure 7 shows the relative error as a function of detected photon number. Open circles represent the (relative) standard deviation of 10 similar YAG pulse measurements, which agrees with the theoretical thermal noise or the shot noise. Note that the theoretical estimates are ambiguous, because we use the nominal values of  $M = 100$ ,  $x = 0.3$  to estimate the

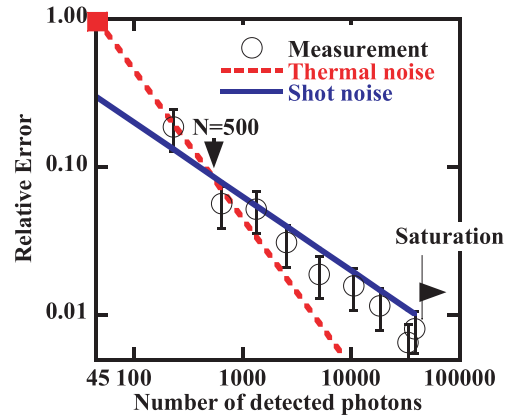


Fig. 7 Relative error of the time-integrated signal (open circles). Theoretical thermal noise (dashed line) and theoretical shot noise (solid line) are also plotted. Filled square represents the (100 %) error with a photon number of 45.

number of detected photons and the shot noise.

## 4. Summary

A bright polychromator for compact, efficient YAG Thomson scattering measurement was designed on the basis of ray-tracing calculations. High refractive index glass (SF11) lenses were used to achieve 98 % efficiency. A fast and low-noise detection system consisting of an APD and two op-amps was designed and tested. The FWHM was 10 ns. The noise was measured and was consistent with theoretical estimations.

## Acknowledgments

This work was supported by Japan Society for the Promotion of Science (JSPS) Grant-in-Aid for Scientific Research No. 21246137 and National Institute for Fusion Science (NIFS) Collaborative Research Program No. NIFS09KUTR039.

- [1] A. Ejiri *et al.*, Nucl. Fusion **46**, 709 (2006).
- [2] S. Kainaga *et al.*, Plasma Fusion Res. **3**, 027 (2008).
- [3] K. Narihara, I. Yamada, H. Hayashi and K. Yamauchi, Rev. Sci. Instrum. **72**, 1122 (2001).
- [4] K. Hanada *et al.*, IEEJ Trans. FM. **129**, 589 (2009).
- [5] J. Cantarini, J. P. Knauer and E. Pasch, Fusion Eng. Des. **84**, 540 (2009).
- [6] R. Pasqualotto *et al.*, Rev. Sci. Instrum. **75**, 3891 (2004).
- [7] A. Alfier and R. Pasqualotto, Rev. Sci. Instrum. **78**, 013505 (2007).
- [8] T. Yamauchi and JFT-2M Experimental Group, Jpn. J. Appl. Phys. **28**, L707 (1989).
- [9] A. Ejiri, T. Oikawa and H. Toyama, Rev. Sci. Instrum. **66**, 4600 (1995).